Physica A xx (xxxx) xxx–xxx

Contents lists available at ScienceDirect

Physica A

journal homepage: www.elsevier.com/locate/physa

Statistical persistence of air pollutants (O_3, SO_2, NO_2 and PM_{10}) in Mexico City

Q1 M. Meraz [a], E. Rodriguez [b], R. Femat [c], J.C. Echeverria [d], J. Alvarez-Ramirez [c,e,*]

[a] *Departamento de Biotecnología, Universidad Autónoma Metropolitana-Iztapalapa, Apartado Postal 55-534, Iztapalapa, 09340 México, Mexico*

[b] *Departamento de Ingeniería Eléctrica, Área de Computación y Sistemas, Universidad Autónoma Metropolitana-Iztapalapa, Apartado Postal 55-534, Iztapalapa, 09340 México, Mexico*

[c] *División de Matemáticas Aplicadas, IPICyT, Camino a la Presa de San José 2055, Lomas 4a Secc, San Luis Potosí, S.L.P., 78290 México, Mexico*

[d] *Departamento de Ingeniería Eléctrica, Área de Ingeniería Biomédica, Universidad Autónoma Metropolitana-Iztapalapa, Apartado Postal 55-534, Iztapalapa, 09340 México, Mexico*

[e] *Departamento de Ingeniería de Procesos e Hidráulica, Universidad Autónoma Metropolitana-Iztapalapa, Apartado Postal 55-534, Iztapalapa, 09340 México, Mexico*

HIGHLIGHTS

- Air-pollutants in Mexico City exhibit long-range persistence.
- Persistence shows scale and time dependences.
- Environmental (daily and yearly) and business (weekly) cycles affect the persistence characteristics.
- Persistence is explained from the self-organized critically framework.

ARTICLE INFO

Article history:
Received 5 August 2014
Received in revised form 18 November 2014
Available online xxxx

Keywords:
Mexico City downtown
Air pollutants
Rescaled range analysis
Persistence

ABSTRACT

The rescaled range (R/S) analysis was used for analyzing the statistical persistence of air pollutants in Mexico City. The air-pollution time series consisted of hourly observations of ozone, nitrogen dioxide, sulfur dioxide and particulate matter obtained at the Mexico City downtown monitoring station during 1999–2014. The results showed that long-range persistence is not a uniform property over a wide range of time scales, from days to months. In fact, although the air pollutant concentrations exhibit an average persistent behavior, environmental (e.g., daily and yearly) and socio-economic (e.g., daily and weekly) cycles are reflected in the dependence of the persistence strength as quantified in terms of the Hurst exponent. It was also found that the Hurst exponent exhibits time variations, with the ozone and nitrate oxide concentrations presenting some regularity, such as annual cycles. The persistence dynamics of the pollutant concentrations increased during the rainy season and decreased during the dry season. The time and scale dependences of the persistence properties provide some insights in the mechanisms involved in the internal dynamics of the Mexico City atmosphere for accumulating and dissipating dangerous air pollutants. While in the short-term individual pollutants dynamics seems to be governed by specific mechanisms, in the long-term (for monthly and higher scales) meteorological and seasonal

* Corresponding author at: División de Matemáticas Aplicadas, IPICyT, Camino a la Presa de San José 2055, Lomas 4a Secc, San Luis Potosí, S.L.P., 78290 México, Mexico. Tel.: +52 55 58044650; fax: +52 55 58044900.
E-mail address: jjar@xanum.uam.mx (J. Alvarez-Ramirez).

http://dx.doi.org/10.1016/j.physa.2015.02.009
0378-4371/

Please cite this article in press as: M. Meraz, et al., Statistical persistence of air pollutants (O_3, SO_2, $NO_2$and PM_{10}) in Mexico City, Physica A (2015), http://dx.doi.org/10.1016/j.physa.2015.02.009

mechanisms involved in atmospheric recirculation seem to dominate the dynamics of all air pollutant concentrations.

1. Introduction

Q2

In the five recent decades, the Mexico City Metropolitan Area (MCMA) has experimented a huge increase of urban limits, population and economic activity. In fact, the population has increased up to more than 20 million inhabitants (about 2556 inhabitants per km^2) and the metropolitan urbanized area has expanded to about 1500 km^2. The combined activity of vehicles and industries consumes more than 45 million liters of petroleum fuel daily, resulting in thousands of tons of pollutants. Moreover, at peak activity hours, the number of on-road vehicles around commercial and industrial zones becomes very large, leading to severe traffic jams and exacerbated emission of primary pollutants. On the other hand, the weather and topographical conditions (e.g., high altitude and tropical insolation) together with the presence of primary pollutants promote the production of secondary contaminants (e.g., ozone), and the formation of high amounts of particulate matter [1]. The continuous exposure to these conditions constitutes a serious threat to the human health quality, with potential negative consequences to economic productivity and city operability [2].

It is recognized that the MCMA is one of the most polluted cities in the world, and so the air pollution problem is a major concern even after the adoption of various control measures such as change in fuel, phasing out of 8 years-old vehicles, shifting of industries to outer areas and lowering of sulfur and benzene content in automobile fuel. The continuous monitoring of major pollutants in diverse stations over the MCMA has indicated that despite the pollutant concentration decrements from the early 1990s, no significant reductions have been obtained in the recent years to fulfill WHO's international standards [1]. In fact, the concentrations of particulate matter, NO_2 and ground O_3 have been maintained stable mainly due to the increase in population and associated traffic density. Among the direct danger for human health, the atmospheric emissions from MCMA contribute to acidification, eutrophication and the occurrence of large-scale pollution haze leading to perturbations of the climate and water cycle [3,4].

The definition of proper public policies for handling the pollution problem in megacities requires an accurate understanding of the mechanisms underlying accumulation and dispersion over short- and long-time horizons. Environmental (e.g., daily and yearly) and socio-economic (e.g., weekly) cycles are known to affect chemical and physical dynamics of pollutants. Basic statistics can provide some insights on the short-time dynamics and long-term trends. However, it is accepted that pollutant dynamics are affected by long-term (e.g., meteorological) and nonlinear (e.g., boundary-layer mixing) mechanisms in such a way that dependences in the long run should be expected. Technically, the interaction of accumulation/dissipation mechanisms can lead to long-term dependences where the short-term dynamics also affect largely the long-term dynamics. On the other hand, the characterization of long-term correlations is an important ingredient to be incorporated within models intended for pollution forecasting, such as classical statistical models (e.g., ARMAX), neural networks [5,6], support vector machines [7], chemistry-transport models [8], among others. Also, the characterization of long-term persistence can provide some insights in the mechanisms involved in the spatial-dependent dispersion of pollutants in urban streets [9].

In principle, the characterization of long-term correlations can be performed with the classical lagged correlation function. However, real time series can be affected by non-stationarities, trends and nonlinearities that can lead to important biased estimations. Since pollutant time series can also meet such features, methods from statistical physics and nonlinear time series analysis have been considered [10]. Along these lines, the most recent methods used for air-pollutant time series analysis include detrended fluctuation analysis [11–13] and rescaled range analysis [13–16]. Long-memory effects in air pollutant concentration dynamics have been detected in those studies. In turn, long-range correlations have been interpreted in terms of self-organizing behavior of the atmospheric system [17]. In particular, these methods provide a
Q3 scaling index that can be interpreted as a measure of the time series predictability in the long term [18]. Persistence analysis can be also used for testing the suitability of proposed models for predicting pollution outcomes since models should reproduce the long-term memory effects observed from field measurements.

The primary task of this work is to explore the long-term statistical dependencies (persistence) of four important pollutants (O_3, SO_2, NO_2 and PM_{10}) in Mexico City downtown. The analysis is based on hourly-sampled time series for the recent 15 years (from 1999 to date). The rescaled range analysis is used to confirm the presence of long-term persistence.

2. Study area

The area under study is the downtown of Mexico City, 19° 25′58.09″ N, 99° 07′59.68″ W. Mexico City is located over a basin with an elevation of 2240 m above sea level. The region is surrounded on three sides by mountain ridges (e.g., Ajusco and Chichinautzin sierras), although a broad Northern opening and a narrower South-Southwest gap are also located at the border of the basin (see Fig. 1(a)). Due to its tropical location and high elevation, Mexico City has a subtropical highland climate (Cwb). The average annual temperature varies from 12 to 16 °C. The temperature is rarely below 3 °C or above 30 °C.

Please cite this article in press as: M. Meraz, et al., Statistical persistence of air pollutants (O_3, SO_2, $NO_2$and PM_{10}) in Mexico City, Physica A (2015), http://dx.doi.org/10.1016/j.physa.2015.02.009

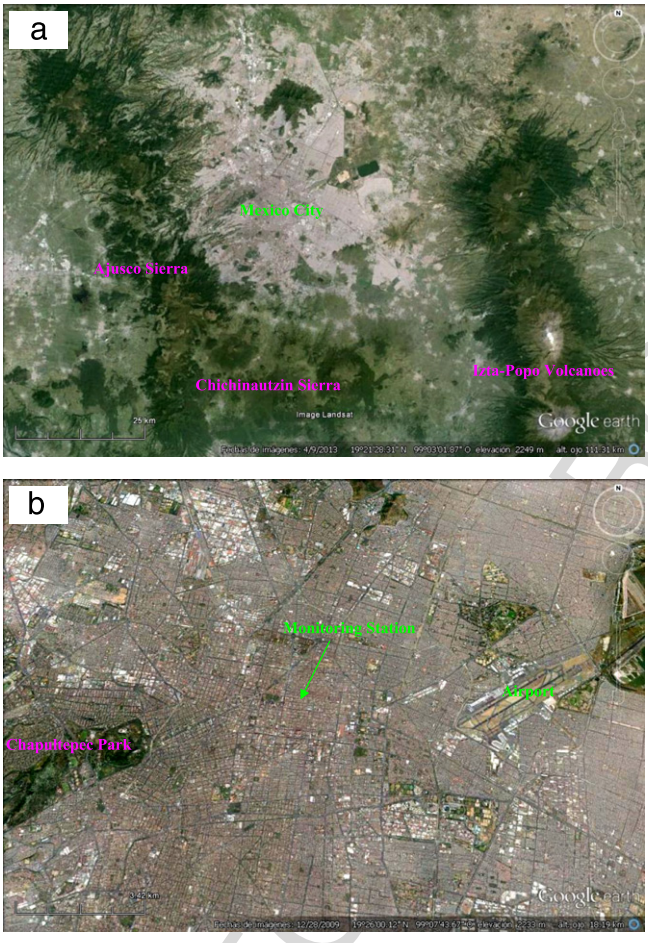

Fig. 1. Google Earth maps showing (a) Mexico City, the mountain ridges and (b) the measuring station.

The area receives about 820 mm of annual rainfall, which is concentrated from June through September/October with little or no precipitation during the rest of the year. The area has two main seasons. The rainy season runs from June to October when winds bring in tropical moisture from the sea. The dry season runs from November to May, when the air is relatively drier.

2.1. Experimental data

The air quality of Mexico City's downtown is monitored continuously in the station located at La Merced site (Fig. 1(b)). Data for the main pollutants (O_3, SO_2, NO_2 and PM_{10}), highlighted by the WHO (www.who.int), are available at the public website www.calidadaire.df.gob.mx, extending from 1999 to date. Observations are reported as hourly mean values. Although monitoring data were also reported for some years before 1999, the data sheets are not complete for those periods. In this way, the present work will consider only the data for the recent 15 years.

3. Methodology

The dynamics of atmospheric contaminants contains both deterministic and stochastic components. The former components are introduced by natural daily, seasonal and yearly cycles. In contrast, stochastic components are introduced by a diversity of factors (economic activity, meteorology, etc.) acting in a complex way. If $X_N = \{x_k\}_{k=1}^{N}$ is a time series of pollutants, an interesting question is related to the existence of long-term correlations in the fluctuating dynamics. The corresponding runoff auto-correlation function $C(s)$ describes how persistence decays in time. If the elements of a time-series x_k are uncorrelated, $C(s)$ is zero for all scales s. If correlations exist only up to a certain number of events s^*, the auto-correlation function will vanish from s^*. By contrast, for long-term correlations, $C(s)$ decays by a scaling power-law $C(s) = \langle x_k x_{k+s} \rangle \approx s^{-\gamma}$. For large values of s, a direct calculation of $C(s)$ can be hindered by noise and by non-stationarities in the data. If the time-series is stationary, one can use standard spectral analysis techniques and calculate the power spectrum $E(f)$ of the time-series as a function of the frequency f. For long-term correlated data, one has that $E(f) \approx 1/f^{\beta}$, where

Please cite this article in press as: M. Meraz, et al., Statistical persistence of air pollutants (O_3, SO_2, $NO_2$and PM_{10}) in Mexico City, Physica A (2015), http://dx.doi.org/10.1016/j.physa.2015.02.009

$\beta = 1 - \gamma$. However, if the time-series is non-stationary, conventional spectral analysis can yield significant bias in the estimation of the correlation strength.

3.1. Rescaled range analysis

The rescaled range (R/S) analysis is a method used to estimate autocorrelation properties of time series. The R/S analysis was developed by Hurst [19], a hydrologist who worked on the problem of reservoir control for the Nile River Dam Project around 1907. Hurst studied the eight and a half-century long records that the Egyptians had kept of the Nile River's overflows. Hurst noted that such records did not appear as a white noise data. Larger-than-average overflows were more likely to be followed by still larger overflows. Abruptly, the process would change to a lower-than-average overflow, which was followed by other lower-than-average overflows. That is, cycles and long-term correlations in the data were manifested. However, standard analysis revealed no statistically significant correlations between observations. In this way, Hurst developed the R/S analysis to distinguish those completely random time series from correlated ones. Rigorous robustness and stability analysis of the R/S method were later provided by Mandelbrot and Wallis [20]. Modern techniques for estimating the Hurst exponent are based on fractal mathematics applied to a large diversity of data, including reservoir modeling [19], markets and financial time series [21], geophysical data [22,23], and cellular biology signals [24], among others. The importance of detecting correlations in time series relies on the fact that these can indicate the presence of deterministic mechanisms driving the dynamics of the underlying stochastic process. In particular, Chamoli et al. [22] have shown the ability of R/S analysis for estimating correlations from short-length sequences.

The main idea behind the R/S analysis is that one looks at the scaling behavior of the rescaled cumulative deviations from the mean, or the distance the system travels as a function of time. For an independent system, the distance covered increases, on average, by the square root of time. If the system covers a larger (resp., smaller) distance, it cannot be independent by definition, and changes must be influencing each other, so that they have to be correlated (resp., anti-correlated). The R/S statistics is the range of partial sums of deviations of sequences from its mean, rescaled by its standard deviation. For a given time series $X_N = \{x_k\}_{k=1}^{N}$, consider a M-dimensional subsequence $Y_M = \{y_k\}_{k=1}^{M} \subset X_N$, where $M < N$. Then, the R/S statistics is estimated by computing the subsample mean $\bar{y}_M = \frac{1}{M}\sum_{k=1}^{M} y_k$, the sequence from partial summations $z_i = \sum_{k=1}^{i}(y_k - \bar{y}_M)$, the range $R_M = \max\{z_i\} - \min\{z_i\}$ and the rescaled range $(R/S)_M = R_M/\sigma_M$, where the sample standard deviation is given by

$$\sigma_M = \left[\frac{1}{M}\sum_{k=1}^{M}(y_k - \bar{y}_M)^2\right]^{1/2}. \tag{1}$$

These steps can be summarized in the following equation [20]:

$$(R/S)_M = \frac{1}{\sigma_M}\left[\max_{1\le i\le M}\sum_{k=1}^{i}(y_k - \bar{y}_M) - \min_{1\le i\le M}\sum_{k=1}^{i}(y_k - \bar{y}_M)\right]. \tag{2}$$

The value $(R/S)_M$ corresponds to the maximum possible distance that a walker can travel with the sequence of steps Y_M. The rescaled range is estimated over a sufficiently large number of non-overlapping sub-vectors (namely, $[N/M]$) Y_M with different sizes or scales M (given in number of events) and then averaged over a sufficiently large number of sample sub-vectors over the whole fractal domain N. The recommended time-scale range is from 10 to $N/5$. If the stochastic process associated to the sequence X_N is scaling over a certain domain $M \in (M_{\min}, M_{\max})$, the R/S statistics follow a power-law

$$(R/S)_M = bM^H \tag{3}$$

where b is a constant and H is the Hurst exponent, which is a fractal-like scaling measurement of the time series auto-correlations. A log–log plot of $(R/S)_M$ as a function of the scale $M \in (M_{\min}, M_{\max})$ gives a straight line with slope H, which is the R/S statistics estimate of the Hurst exponent. In case of having only short-range correlations (or no correlations at all) the walk profile displays properties of a standard random walk (*e.g.*, white noise) with $H = 0.5$. If $H > 0.5$ the correlations in the signal are *persistent* (*i.e.*, an increment is very likely to be followed by an increment, and a decrement by a decrement). The value $H = 1.0$ corresponds to $1/f$-noise, a flicker noise that commonly appears in nature. On the other hand, if $H < 0.5$ the auto-correlations in the signal are *anti-persistent* (*i.e.*, an increment is very likely to be followed by a decrement) indicating the presence of oscillations. The case $H \to 0$ corresponds to periodic (*e.g.*, harmonic) signals. The fractal dimension of a time series is related to its Hurst exponent by means of the relationship $D_{fr} = 2 - H$.

3.2. Scale-dependent Hurst exponent

In some cases, a unique power-law might not fully describe the behavior of the fluctuations function $(R/S)_M$. That is, the log–log slope of the fluctuation function $(R/S)_M$ presents a continuous change that depends on the scale M. This feature is interpreted as if the Hurst exponent of the time-series is scale-dependent. Given the plot of $\log(R/S)_M$ versus $\log(M)$,

Please cite this article in press as: M. Meraz, et al., Statistical persistence of air pollutants (O_3, SO_2, $NO_2$and PM_{10}) in Mexico City, Physica A (2015), http://dx.doi.org/10.1016/j.physa.2015.02.009

a procedure for computing the local slope should be implemented. For reducing the effects of numerical instabilities that commonly affect the numerical computation of derivatives, and for detecting patterns in the scaling behavior of the pollutant fluctuations, an alpha–beta filtering strategy was used [25]. Specifically, for a given sequence y_k, $k = 1, 2, \ldots, N_R$, the alpha–beta filtering is based on a mechanical system analogy, with two states that are called position y and velocity v. Assuming that velocity remains approximately constant over the small distance Δx between measurements, the position and velocity states are projected forward to predict its value at the next sampling time using the following equation:

$$\begin{aligned} y_{k+1}^{est} &= y_k^{est} + \alpha r_k \\ v_{k+1}^{est} &= v_k^{est} + \left(\frac{\beta}{\Delta x}\right) r_k \end{aligned} \tag{4}$$

where $r_k = y_k - y_k^{est}$ is the residual or innovation. For the estimation of the local slope from the R/S analysis, the sequence y_k corresponds to the logarithm of $(R/S)_M$, while the resulting estimated velocity v_k^{est} is the estimated local slope at the kth position. The parameters α and β are introduced for smoothing purposes. For convergence, stability and noise suppression, the values of the α and β multipliers should be positive and small; namely, $\alpha \in (0, 1)$ and $\beta \in (0, 1)$. In general, larger α and β gains tend to produce faster response for tracking transient changes, while smaller α and β gains reduce the level of noise in the state estimates. If a good balance between accurate tracking and noise reduction is found, and the algorithm is effective, filtered estimates are more accurate than the direct measurements. The values $\alpha = 0.5$ and $\beta = 0.1$ provide acceptable accuracy for the estimation of the Hurst exponent [25]. The procedure results in an estimated Hurst exponent as a function of the scale, $H(s)$, where $s = \Delta t M$ and Δt is the sampling period.

The computation of the scaling exponent for the specific time weekly, monthly and quarterly periods was performed with the alpha–beta filtering strategy described above. For these periods, the corresponding time scale s was taken as 168, 720 and 2160 hourly observations. The local scaling exponent reflects the slope of the function $(R/S)_M$ at the distinguished scales.

3.3. Time-dependent Hurst exponent

Real stochastic processes can exhibit temporal changes due to, e.g., exogenous disturbances and structural changes. In this way, it is very likely that the auto-correlations properties of the underlying time-series are dependent of the time. For detecting temporal changes in the Hurst exponent, the R/S analysis can then be implemented within a rolling window framework [26]. Briefly, for a given time series, the R/S algorithm described above was implemented over sub-time series obtained from a rolling window of size N_r. For data extracted from the rolling window, the local scaling exponent is obtained by the application of the alpha–beta filtering. In this way, one obtains a time series $H(t)$ corresponding to the temporal variations of the Hurst exponent over daily, weekly and quarterly time scales.

4. Results and discussion

4.1. Primary analysis

The WHO has remarked the health risks when air pollutant concentrations are above certain threshold values. According to the guidelines by the WHO, the maximum allowable values for air pollutants are the following:

(a) *Ozone* (O_3): 100 $\mu g/m^3$ over an 8 h mean. Above this value, ozone becomes a serious risk for asthma morbidity and mortality.
(b) *Sulfur dioxide* (SO_2): 20 $\mu g/m^3$ over a 24 h mean. Sulfur dioxide plays a role in asthma, bronchial symptoms, lung inflammation and reduced lung function.
(c) *Nitrogen dioxide* (NO_2): 200 $\mu g/m^3$ over a 1 h mean. Nitrogen dioxide becomes a risk for asthma and reduced lung function.
(d) *Small particles*(PM_{10}): 50 $\mu g/m^3$ over a 24 h mean. The major components of PM_{10} are sulfate, nitrates, ammonia, sodium chloride, black carbon, mineral dust and water. Chronic exposure to particles contributes to the risk of developing cardiovascular and respiratory diseases, as well as of lung cancer.

Fig. 2 exhibits the pollutant time series for the four air pollutants described above. For comparing with the threshold values indicated by the WHO guidelines, the time series were moving averaged over the specific time windows (e.g., 8 h as suggested for ozone). The horizontal dotted line corresponds to the WHO's maximum allowable value, while the vertical gray strips indicate the winter–spring annual period. The following comments can be drawn from the data depicted in Fig. 2: (a) Thanks to the implementation of public policies dating from the early 1990s, except for PM_{10}, the concentration of air pollutants showed a gradual decrease. However, it is apparent that the concentrations achieved a stationary, non-decreasing pattern by 2007. (b) The ozone concentrations are continuously higher than the WHO's maximum allowable values, with concentrations peaks in the summer–autumn (i.e., rainy) period. (c) Sulfur dioxide exhibits an annual cycle, with concentrations peaks in the winter–spring (i.e., dry) period. In general, for those years after 2007 the WHO's maximum allowable value is satisfied only in the summer–autumn period. (d) Nitrogen dioxide also presents an annual cycle with concentration peaks in the spring–summer period. Interestingly, the nitrogen dioxide concentration is always within the

Please cite this article in press as: M. Meraz, et al., Statistical persistence of air pollutants (O_3, SO_2, $NO_2$and PM_{10}) in Mexico City, Physica A (2015), http://dx.doi.org/10.1016/j.physa.2015.02.009

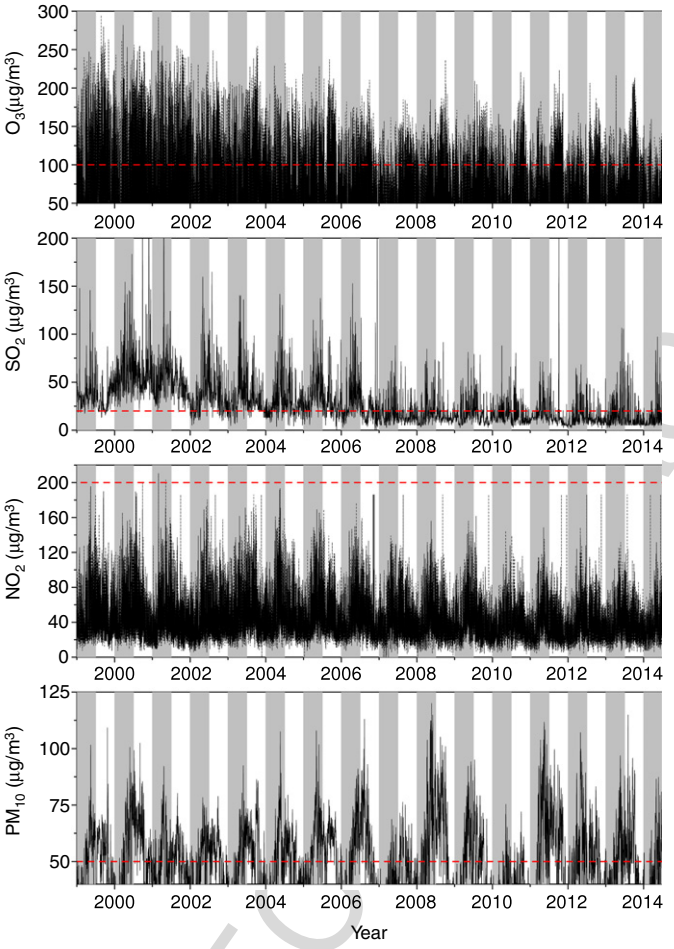

Fig. 2. Concentration behavior of four air pollutants in Mexico City downtown. The dotted red line corresponds to the maximum allowable concentration according to the WHO's guidelines. Except for the nitrogen dioxide, the other three pollutants seem out of specifications despite the gradual decrease showed up to 2007.

WHO's recommendations. (e) In contrast to other air pollutants that showed a gradual decrease, the peak values of small particle concentration exhibit a positive trend, mainly after 2007. The peak concentrations are found mainly in the dry–rainy transition (i.e., spring–summer period), when the WHO's recommendation is not satisfied. Summing up, although air pollutants showed a gradual decrease in the 1990s and early 2000s, their concentration pattern has achieved a stationary value that is commonly higher than the WHO's recommendations. The worst scenario is presented by small particles that present a positive concentration trend. Given the serious risks that the pollutant levels impose for human health, an interesting question is to characterize the dynamics of concentration fluctuations along the recent years.

4.2. *R/S* analysis

The pollutant time series are affected by long-term trends and seasonalities, mainly for yearly and daily scales. For instance, Fig. 3(a) presents the yearly trend for the NO_2 time series. The presence of a one-year cycle can be clearly observed. As already commented, the yearly variations of this pollutant exhibited a slight decrease from 1999 to 2007. Afterwards, the yearly cycle seems to be stabilized about a stationary pattern. As a preliminary step for assessing the statistical persistence of the pollutants, the effects of the season trends in the Hurst exponent were evaluated. To this end, the yearly trend in Fig. 3(a) was removed from the raw data and subsequently the R/S analysis was applied. Fig. 3(b) compares the results of the R/S analysis for the raw and the detrended time series for yearly and daily trends. The removing of the yearly trend affects the R/S results for relatively high time scales, while the R/S function for smaller time scales remains unchanged. In contrast, removing the daily trend affects the R/S computations for time scales higher than one day. In fact, the one-day detrending of the time series removes the long-term pollutant fluctuations. In this way, the removing of the long-term fluctuations for a given time horizon allows the evaluation of the statistical persistence only for time scales smaller than the detrending time horizon. Since we are interested in exploring the statistical persistence for time scales from days to weeks, and given that

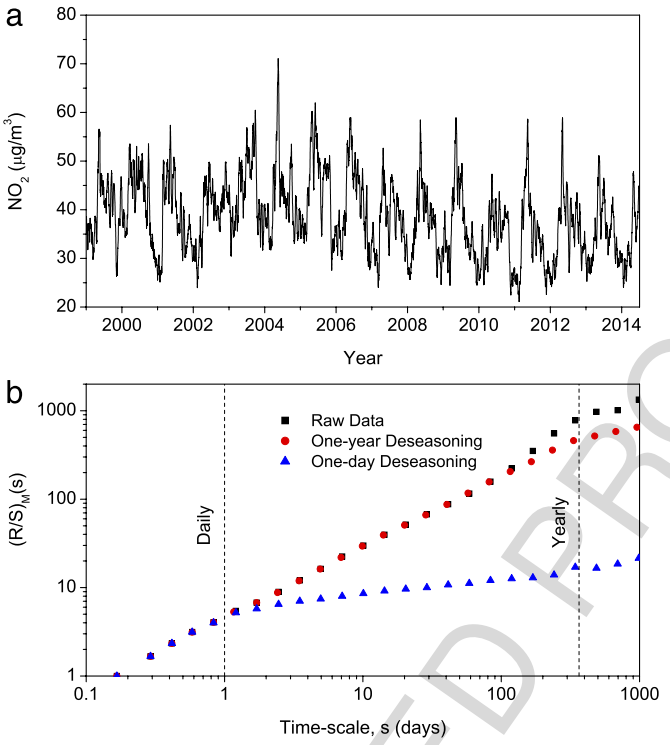

Fig. 3. (a) Long-term trend and yearly seasonality of the nitrogen dioxide concentration. (b) R/S analysis results for the raw time series and for the detrended time series by removing yearly and daily seasonalities.

the yearly seasonality affects only large time scales, the R/S analysis was applied directly in the original time series. Besides, for reducing the possible bias induced by long-term trends and yearly seasonality, the statistical persistence, estimated in terms of the Hurst exponent, was constrained for time scales smaller than one quarter.

A major problem with the R/S method is its sensitivity to short-term memory effects [27]. For instance, it should be clarified whether a given time series is indeed long-term correlated or just short-term correlated with a fairly large correlation time scale. That is, the R/S analysis may be biased by short-term Markovian dependence. Davis and Harte [28] showed that conventional R/S analysis using a Hurst regression can be biased toward accepting a long-term dependence hypothesis even when the true process is first-order autoregressive. Maraun et al. [29] indicated that the spurious propagation of short-term correlations into long time-scales should be discarded. To this end, it was proposed to reject the exponential decay of the autocorrelation function and to show the constancy of local slopes. The auto-correlation function $C(\tau)$ describes how persistence decays in time. If the elements of a time-series x_k are uncorrelated, $C(\tau)$ is zero for all lags τ. If correlations are only of short-term nature, the auto-correlation function $C(\tau)$ will show an exponential decay. In contrast, for long-term correlations, $C(\tau)$ decays as a scaling power law $C(\tau) = \langle x_k x_{k+\tau} \rangle \approx \tau^{-\gamma}$. For the NO_2 time series, Fig. 4(a) illustrates the behavior of the auto-correlation function over a wide range of time-scales. It can be noted that the numerical results cannot follow a power-law behavior $C(\tau) \approx \tau^{-\gamma}$ for time scales from 0.1 to 300 days. It should be pointed out that similar results were obtained for the other three pollutant time series. This suggests that the time series of pollutants is affected by long-term correlations. For correcting potential short-term effects, Tabak and Cajueiro [30] proposed to apply the R/S analysis to blocks of shuffled data. This procedure is carried out by picking a random permutation of the data series within non-overlapping blocks of predetermined small-size blocks and applying the R/S analysis to this shuffled data. In this way, the effect of random permutations in these small blocks is the destruction of any particular structure of auto-correlation in the data contained in the blocks. Also for the NO_2 time series, Fig. 4(b) exhibits the effect of the block-shuffling in the function $(R/S)_M$. Shuffling over blocks of 24 observations, corresponding to a day, the function is affected only weakly for intraday time scales, while the behavior for higher time scales is not affected. This suggests that short-term correlations are not masking the possible existence of long-term persistence. Applying shuffling for larger block sizes should destroy the structure of the function $(R/S)_M$ for time scales smaller than the corresponding for the block size. In fact, the shuffling for blocks of size of one month deploys the R/S results for time scales smaller than about 12 days. In the limit when the whole time series is shuffled, the Hurst exponent of the shuffled R/S results is about 0.5, indicating non-correlated dynamics. Besides the power-law decay of the auto-correlation function in Fig. 4(a), the convergence of the Hurst exponent to about 0.5 for the fully shuffled data suggests that the detected long-term persistence is an intrinsic property of the original time series and not an artifact of the short-term correlations. Also, the power-law behavior of the R/S results is obtained from the internal order of the pollutions time series, and not of the extreme events linked to fat-tailed distributions. In order to

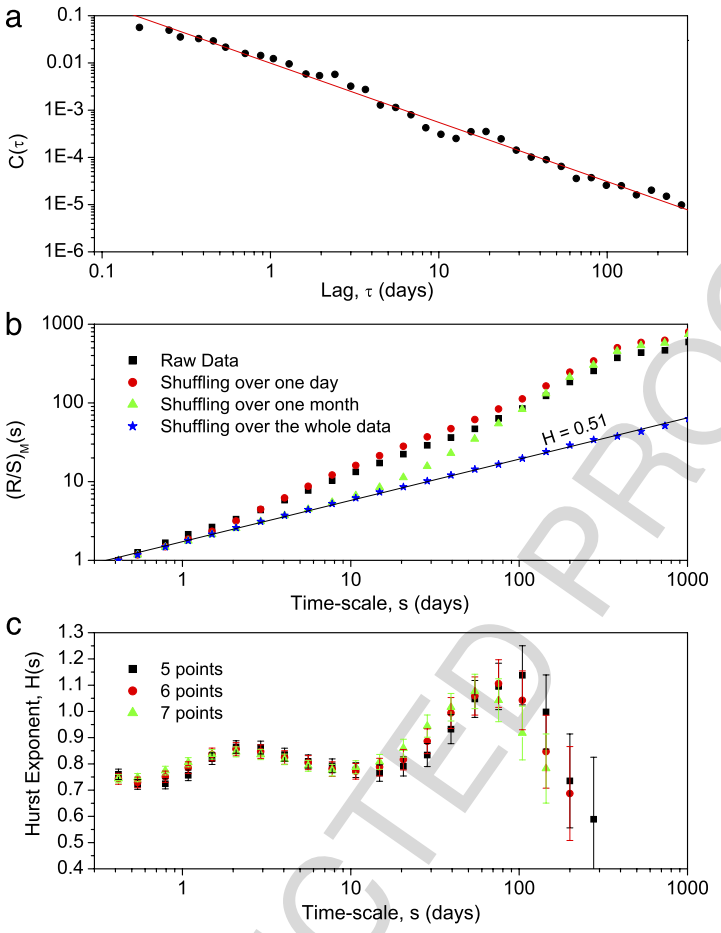

Fig. 4. (a) Correlation function $C(\tau)$ over a wide range of lags τ. Note that $C(\tau)$ exhibits a power-law behavior, which is reflecting the presence of long-term correlations. (b) Results of the R/S analysis for different shuffling windows. The Hurst exponent converges to 0.5 when the whole data are shuffled. (c) Local slope as function of the size of the fitting window.

clarify the limits of how close to the uncorrelated noise the data are and the underlying level of confidence, the local slope (i.e., the Hurst exponent as function of the time scale) was estimated [29,31,32]. First, a straight line was fitted to $\log(R/S)_M$ versus $\log(s)$ within a small window, which was shifted successively over all scales. Fig. 4(c) exhibits the local slope and the estimated variance for three different sizes of the fitting window. For small time scales, the variance is low and for higher time scales the variance is increased. The increased variance for high time scales is possibly caused by the reduced number of non-overlapping boxes used for computing the R/S range $(R/S)_M$. However, the results in Fig. 4(c) show that the estimation of the local slope is stable with respect to the number of fitting points, while presenting a regular range of constancy. This analysis supports the finding in Fig. 3(a) where the power-law decay of the autocorrelation function cannot be discarded.

The results in Fig. 3 indicated that the pollutant time series contain long-term persistence effects that are displayed at different time scales, from days to weeks. Although the NO_2 was used for illustrating the statistical stability of the R/S analysis, the other three time series exhibit similar results. For time scales from 0.25 to 1000 days, Fig. 5(a) presents the results of the R/S analysis for the four pollutants described above with the lines representing the least-square power-law fitting for the power-law equation (3). All the pollutants exhibited persistent behavior with PM_{10} and ozone presenting the highest (0.904 ± 0.005) and the lowest (0.765 ± 0.012) Hurst exponent values. Persistence means that a pollutant concentration pattern in one particular time continues into the next. In this way, high persistence implies a strong correlation between successive data points in the sense that the pollutant concentration pattern is statistically similar. The results in Fig. 5(a) indicate that PM_{10} exhibits stronger long-term correlations than the other three pollutants, and these correlations prevail over a wide range of time scales, from hours to years.

4.2.1. Scale-dependent persistence

The $(R/S)_M$ response in Fig. 5(a) was fitted by a power-law function $(R/S)_M = bM^H$ for time scales from hours to years. However, some important deviations from a uniform power-law behavior can be noted. For instance, the ozone case exhibits positive deviations for daily and yearly time scales, and negative deviations for time scales in the range from 7 to 120 days.

Please cite this article in press as: M. Meraz, et al., Statistical persistence of air pollutants (O_3, SO_2, $NO_2$and PM_{10}) in Mexico City, Physica A (2015), http://dx.doi.org/10.1016/j.physa.2015.02.009

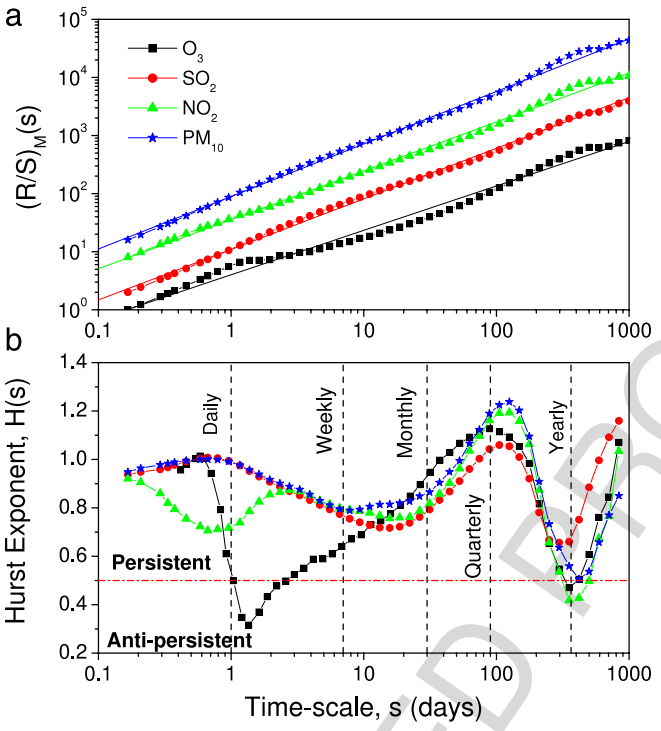

Fig. 5. Results of the R/S analysis for the four pollutants described in Fig. 2. (a) The lines represent the least-square power-law fitting for the power-law equation (3). (b) All the pollutants exhibited persistent behavior, with PM_{10} and ozone presenting the highest (0.904 ± 0.005) and the lowest (0.765 ± 0.012) Hurst exponent values.

This suggests that a sole power-law fitting does not suffice for describing the scaling properties of the pollutant fluctuations. In turn, this means that the Hurst exponent should be considered as a function of the time scale. Alpha–beta filtering can be used for computing the local slope of the log–log plot of the function $(R/S)_M$ [25]. The results of the scale-dependent Hurst exponent, $H(s)$, are exhibited in Fig. 5(b) for the four pollutant concentrations. The following salient features can be commented:

(a) *Ozone* (O_3): The Hurst exponent presents two minimum values at time scales of about one day and one year. In turn, these Hurst exponent values reflect the daily and yearly cycles of the concentration dynamics of this pollutant. The daily cycle is related to anti-persistent dynamics ($H \approx 0.3$), indicating that a today's high (resp., low) concentration is likely to be followed by a low (resp., high) concentration. In this way, the dynamics of the ozone concentration involves day-to-day dissipation mechanisms that alleviate the accumulation effects in subsequent days. In contrast, the Hurst exponent for the yearly cycle is about 0.5, reflecting the lack of long-term correlations within this time scale. That is, the ozone concentration pattern for time scales of about one year cannot be easily predicted since its behavior is linked to random, uncorrelated dynamics. Strong correlations ($H \approx 1.15$) are found for time scales of about 90 days, indicating a high degree of persistence for quarterly time horizons. Differences in the predictability of ozone concentration with respect to the time scale were also observed for ground level pollution dynamics in Dheli [33]. For instance, statistical persistence nature is observed for the ozone concentration with 1 and 4 h frequency, whereas at 8 and 24 h time scale, the ozone concentration shows random behavior.

(b) *Sulfur dioxide* (SO_2): The sulfur dioxide dynamics does not exhibit a clear daily pattern as reflected by the relatively high value ($H \approx 1.0$) Hurst exponent for intra-day and intra-week time scales. Interestingly, the Hurst exponent value $H = 1.0$ corresponds to 1/f-noise, a behavior occurring in many physical, biological and economic systems. The importance of 1/f-noise is that it exhibits a subtle balance between stochastic and deterministic components. The Hurst exponent exhibits a minimum value ($H \approx 0.65$) at about 310 days, which could be reflecting the effects of the yearly cycle. In such case, the Hurst exponent is related to relatively weak persistence, and so to some degree of pattern predictability.

(c) *Nitrogen dioxide* (NO_2): The nitrogen dioxide dynamics exhibits a local minimum of the Hurst exponent at about 0.75 days, which can be related to the daily cycle. However, in contrast to the ozone concentration, the daily Hurst exponent reflects persistence dynamics, and so the absence of a daily dissipation process. That is, the nitrogen dioxide is not completely dissipated along the daily cycle, exhibiting accumulation waves over the subsequent days. The yearly cycle is clearly reflected by the presence of the minimum Hurst exponent value ($H \approx 0.4$) for scales of about 365 days.

Please cite this article in press as: M. Meraz, et al., Statistical persistence of air pollutants (O_3, SO_2, $NO_2$and PM_{10}) in Mexico City, Physica A (2015), http://dx.doi.org/10.1016/j.physa.2015.02.009

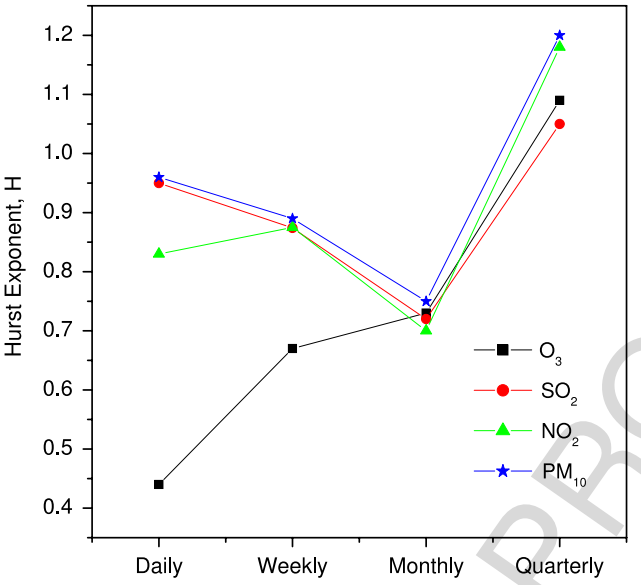

Fig. 6. Hurst exponent values corresponding to four different time scales. It is noted that the Hurst exponent for the four air pollutants converge to about 0.72 for the monthly time scale.

Anti-persistence in the yearly dynamics is then apparent, which could be reflecting the dissipation effects by long-term meteorological conditions.

(d) *Small particles* (PM_{10}): Interestingly, for time scales up to one week, small particles exhibit the same Hurst exponent pattern than sulfur dioxide. This could be suggesting a coupling of the dynamics of these two pollutants for weekly scales. Interestingly, weekly scales are related to the socio-economic dynamics with 5.5 days of intense industrial and vehicular activities and the remaining 1.5 days (Saturday afternoon and Sunday) of reduced activity. It has been found that sulfur compounds are among the largest fractions, via secondary aerosols, of PM_{10} composition [34,35]. The yearly cycle is reflected by the Hurst exponent minimum ($H \approx 0.5$) at about 365 days, indicating that the pattern of the small particle concentration is unpredictable for yearly time scales. The maximum Hurst exponent value ($H \approx 1.2$) at about 120 days suggests that meteorological seasonality can be affecting the dynamics of the PM_{10} concentration.

Summing up, the results in Fig. 5(b) indicated that: (i) All pollutants in Mexico City downtown are affected by a yearly cycle with dynamics similar to random behavior. (ii) Only the ozone concentration exhibited a clear daily cycle. (iii) The maximum exponent value, and hence maximum predictability, is found for time scales of about 90–120 days, suggesting that meteorological seasonality affects largely the persistence of the pollutants. (iv) For time scales smaller than about one month, the four pollutants exhibit different dynamics as indicated by values of the Hurst exponent. However, the Hurst exponent behavior tends to converge to a unique pattern for time scales higher than about one month. Fig. 6 presents the Hurst exponent value for daily, weekly, monthly and quarterly time scales. A pinch point can be observed for the monthly time scale, which could indicate that the dynamics of pollutants accumulation are governed by the same mechanism after one month. While ozone concentration is strongly affected by daily dynamics, it is apparent that some large scale mechanisms, like atmospheric mixing, over long time determines the behavior of all pollutants in Mexico City downtown. For smaller time scales, the mechanisms underlying the pollutant dynamics are specific for each chemical component.

4.2.2. Time-dependent persistence

It has been shown that the fluctuations of pollutant concentrations do not follow a uniform power-law behavior according to the R/S analysis. In fact, for the scrutinized period 1999–2014, the fluctuations exhibited a Hurst exponent that depends of the temporal scale. In turn, such dependency can be linked to accumulation/dissipation mechanisms acting at different time scales. A further interesting issue is how the persistence, quantified in terms of the Hurst exponent, has changed along recent years. For addressing this point, the R/S analysis was implemented over a half-year (4380 observations) rolling window. Similar to time–frequency (e.g., wavelet) analysis, one can obtain a Hurst exponent that depends on both time and scale, $H(t, s)$. Fig. 7(a)–(d) present the Hurst exponent color map for ozone, sulfur dioxide, nitrogen dioxide and small particles, respectively. The non-uniformity of the persistence properties for all pollutants can be observed. In fact, the Hurst exponent exhibits important time variations with time. The effect of the daily anti-persistent cycle for ozone is displayed as the horizontal blue band corresponding to a Hurst exponent of about $H \approx 0.1$. The daily cycle is also displayed by nitrogen dioxide, although with weaker anti-persistence features. For all pollutants, strong persistence bands are exhibited for higher time scales, from weeks to months. This corroborates the results presented in Fig. 5 that showed that pollutant fluctuations

Please cite this article in press as: M. Meraz, et al., Statistical persistence of air pollutants (O_3, SO_2, $NO_2$and PM_{10}) in Mexico City, Physica A (2015), http://dx.doi.org/10.1016/j.physa.2015.02.009

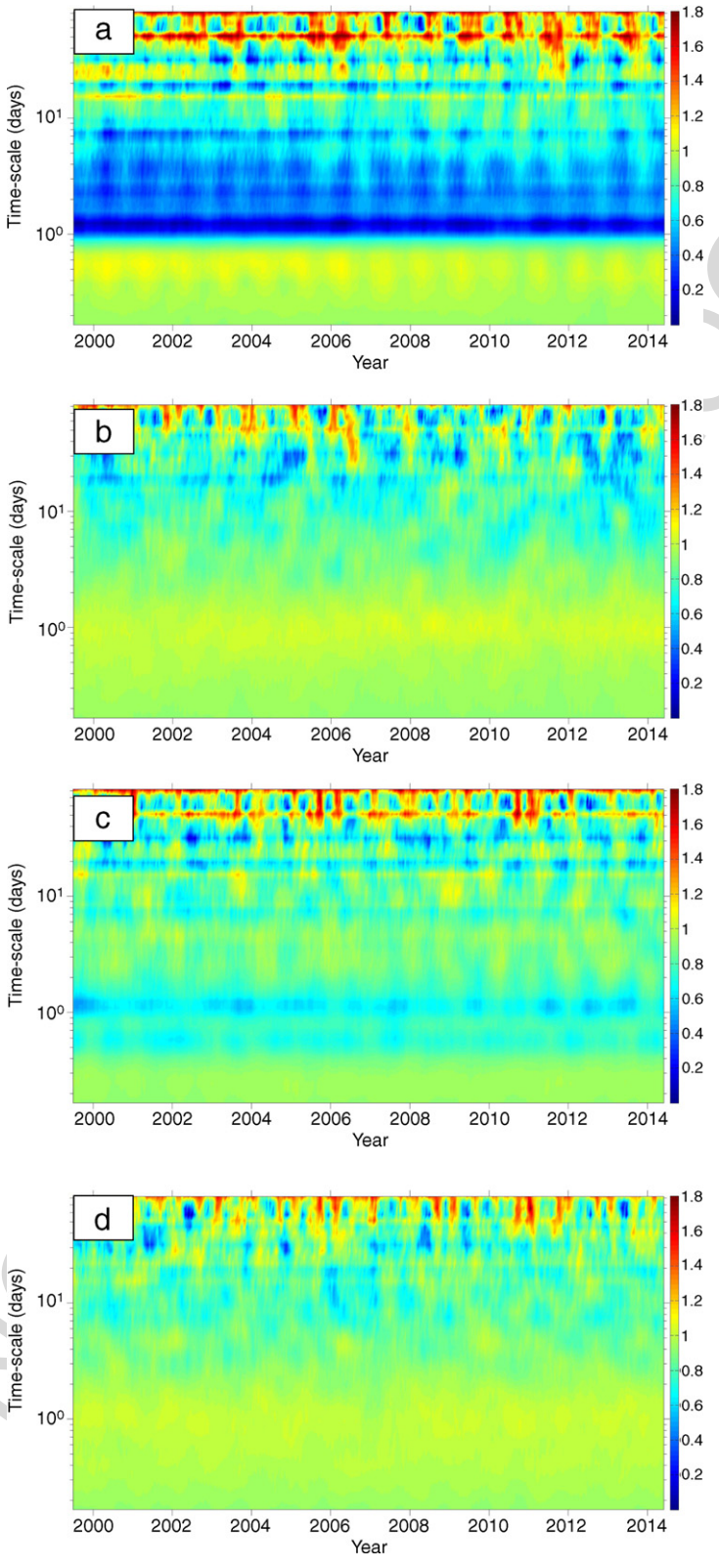

Fig. 7. Hurst exponent as function of time and temporal scale for (a) ozone, (b) sulfur dioxide, (c) nitrogen dioxide, and (d) particulate matter. Similar to a (time–frequency) wavelet analysis, the color map shows the scales at which the specific air-pollutant exhibits highest persistence.

Please cite this article in press as: M. Meraz, et al., Statistical persistence of air pollutants (O_3, SO_2, $NO_2$and PM_{10}) in Mexico City, Physica A (2015), http://dx.doi.org/10.1016/j.physa.2015.02.009

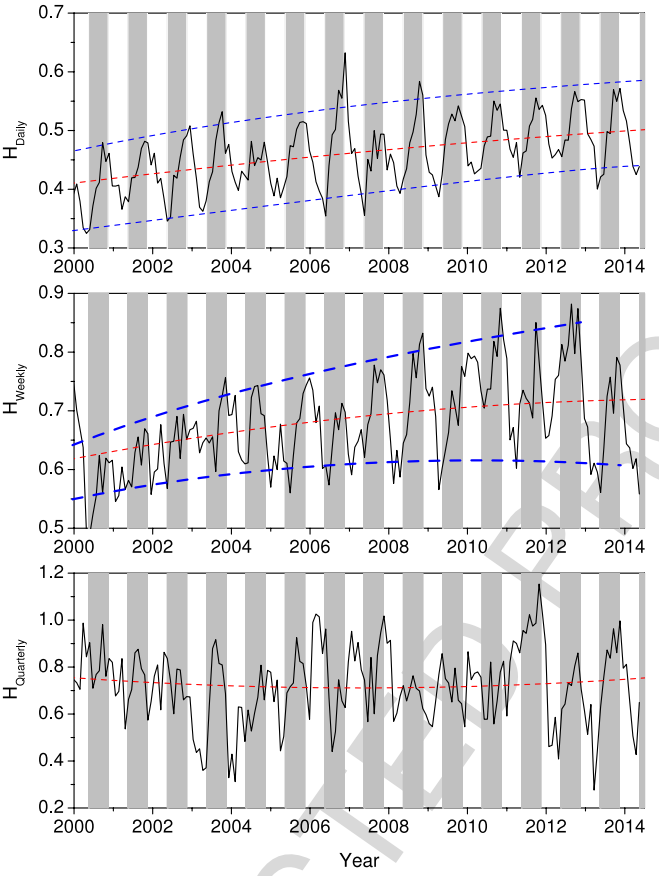

Fig. 8. Time variations of the Hurst exponent for ozone concentration over three different scales. It can be noted the presence of an annual cycle for daily and weekly scales.

in Mexico City downtown can remain for long times. That is, large concentration fluctuations in current days should have strong effects in the air pollution pattern for the coming next weeks.

For a more detailed analysis of the Hurst exponent pattern in Fig. 7, the time variations of the Hurst exponent for three important time scales were considered; namely: (i) Intraday scales, which contain the basic mechanisms of pollutant generation and dissipation. For instance, ozone concentration follows a daily cycle driven by photo-catalyzed reactions. To this end, intraday scales were considered by averaging the Hurst exponent over time scales in the range from 12 to 24 h. (ii) Weekly scales are important since socioeconomic dynamics are conformed within weekly patterns. In general, vehicular and industrial activities are higher during working days and lower during weekends. (iii) Quarterly scales are related to meteorological seasons. As mentioned earlier, Mexico City has two main seasons. Although there is some variation in temperature over the year, the most obvious difference is between rainy (mid-May through September or mid-October) and dry seasons. During the rest of the year there is little or no rain at all. The results of the rolling window Hurst exponent analysis can be described and commented as follows:

(a) *Ozone* (O_3): The results for ozone are displayed in Fig. 8 where the gray and white vertical bars correspond to the rainy and dry season, respectively. For the daily time scale, the Hurst exponent exhibits an annual cycle with the mean trend (red dotted line) increasing gradually from about 0.4 in 1999 to about 0.5 in 2014 for. This implies that, on average, the ozone concentration behavior is becoming more random and, hence, less predictable. Interestingly, the upward phase of the Hurst exponent cycle coincides with the rainy season, while the downward phase with the dry season. In other words, the persistence of ozone increases during the rainy season and decreases during the dry season. It is suggested that during the wet season, high atmospheric humidity and rain become the dominant driving mechanisms for the ozone concentration dynamics. In contrast, the formation of strong surface-based inversions at night, persisting several hours after sunrise, reduces the predictability of the ozone concentration outcomes. It is noted that the annual cycle in the Hurst exponent is also apparent for weekly time scales. An interesting feature is that the cycle amplitude is also increasing gradually (blue dotted line). Besides, the upward and downward phases of the annual cycle coincide with the rainy and dry seasons, respectively. The Hurst exponent for quarterly time scale exhibits a less regular pattern, with some peaks located within the rainy season. On average, the quarterly Hurst exponent has remained nearly constant at about 0.65; however, large variations between persistence and anti-persistence are also exhibited. The irregular pattern of the

Please cite this article in press as: M. Meraz, et al., Statistical persistence of air pollutants (O_3, SO_2, $NO_2$and PM_{10}) in Mexico City, Physica A (2015), http://dx.doi.org/10.1016/j.physa.2015.02.009

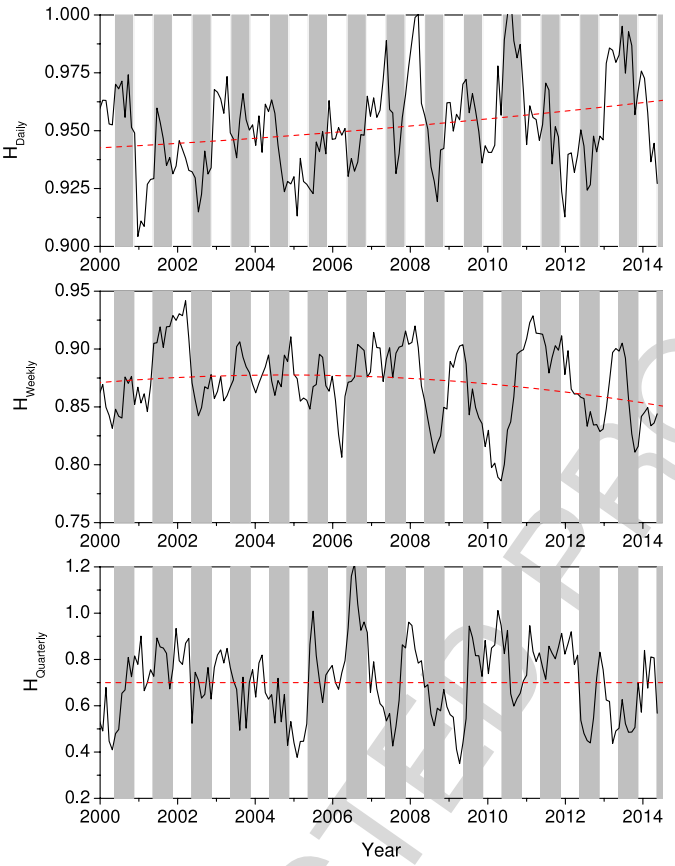

Fig. 9. Time variations of the Hurst exponent for sulfur dioxide concentration over three different scales. In contrast to the ozone concentration, the presence of an annual cycle in the Hurst exponent variations is not observed.

quarterly Hurst exponent might be related to long-term meteorological conditions affecting the winds, humidity and temperature in Mexico City downtown.

(b) *Sulfur dioxide* (SO_2): The time variations of the Hurst exponent for sulfur dioxide are presented in Fig. 9. In contrast to the ozone concentration, the sulfur dioxide does not show an annual cycle of the Hurst exponent. In fact, for daily, weekly and quarterly scales the Hurst exponent exhibits irregular variations about a nearly constant mean value. Although the sulfur dioxide concentration showed a gradually decreasing behavior from 1999 to about mid-2006, the mean concentration has been maintained for the recent seven years (Fig. 2(b)). However, this feature has not been reflected in the predictability of the sulfur dioxide fluctuations at any time scale. The lack of regularity in the Hurst exponent for sulfur dioxide suggests the involvement of many mechanisms interlaced in a complex way.

(c) *Nitrogen dioxide* (NO_2): The results of the Hurst exponent variations over time for nitrogen dioxide are presented in Fig. 10. Similar to the ozone concentration, the Hurst exponent exhibits an annual cycle for daily and weekly time scales. This is not surprising at all since ozone and nitrogen oxide are interlinked via the oxidation of nitrogen monoxide, NO_2; a pollutant resulting mainly from combustion engines, wastewater treatment plants and agriculture fertilizers. An important difference with ozone is that the Hurst exponent variations are always located within the persistence region (i.e., $H > 0.5$) for the three time scales. Also, while the Hurst exponent peak for ozone is located at the rainy–dry season transition (Fig. 8), the corresponding peak for nitrogen oxide is located at the middle of the dry season. Fig. 11 compares the behavior of the Hurst exponent cycle for ozone and nitrogen dioxide in the recent six years. The phase lag between the ozone and nitrogen annual cycles is about 0.25 years, corresponding to a meteorological season. In this way, high persistence of ozone concentration is associated, except for 2010, with a low persistence of nitrogen oxide concentration.

(d) *Small particles* (PM_{10}): The Hurst exponent variations for small particles are shown in Fig. 12. An annual cycle seems to be present for daily and weekly scales. The most interesting feature is displayed for daily time scale. The persistence exhibited a gradual decrease of the mean value (red dotted line) for the period from 1999 to 2006. In 2007, the Hurst exponent exhibited a sudden increase from about 0.9 to 0.96 and remained higher from that value onwards, suggesting an unsuspected link between small and large events. It is apparent that the dynamics of the small particle concentration was affected by some events occurring in 2007, such as the starting-up of new vehicle transit lanes over the city highway ring, the adoption of various transit control measures or the implementation of more restrictive sulfur content in fuels.

Please cite this article in press as: M. Meraz, et al., Statistical persistence of air pollutants (O_3, SO_2, $NO_2$and PM_{10}) in Mexico City, Physica A (2015), http://dx.doi.org/10.1016/j.physa.2015.02.009

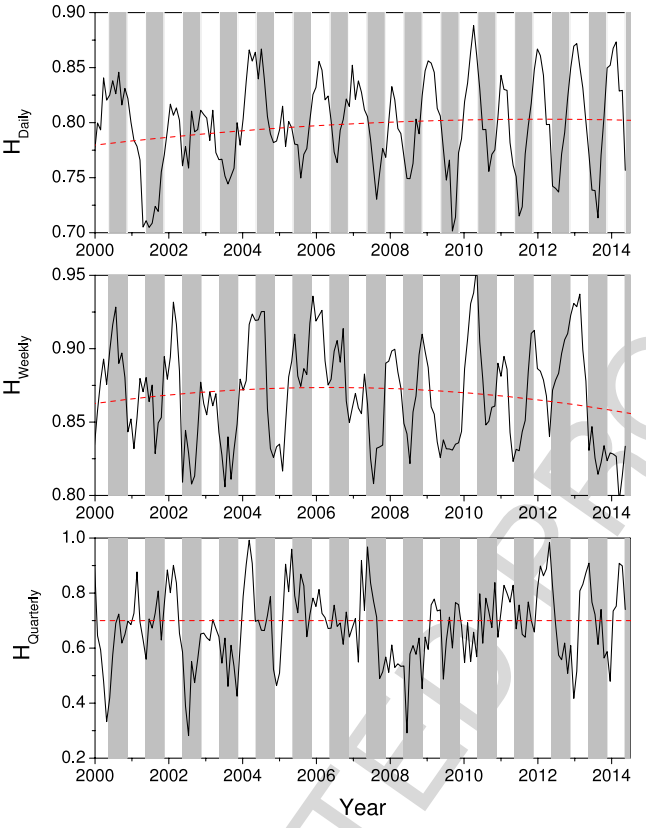

Fig. 10. Time variations of the Hurst exponent for nitrogen dioxide concentration over three different scales. Similar to ozone concentration, the Hurst exponent for nitrogen oxide concentration exhibits an annual cycle over daily and weekly time scales.

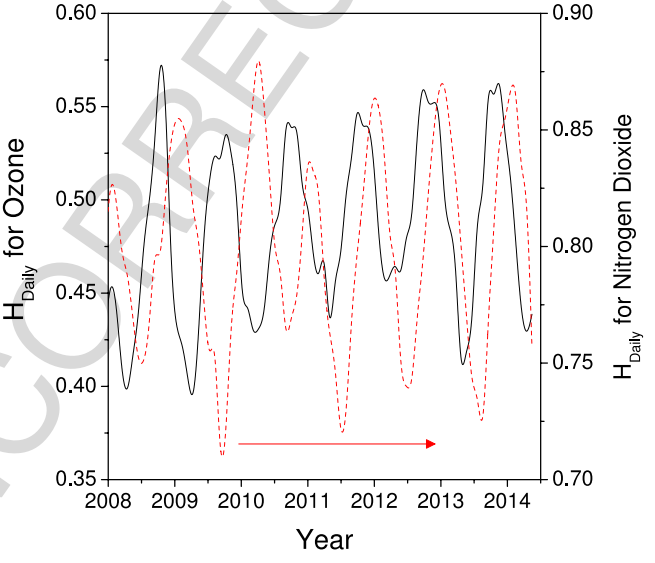

Fig. 11. Comparison between the daily Hurst exponent for ozone and nitrogen dioxide concentration for the recent seven years. A phase lag of about 0.25 years between the annual cycles can be observed for the recent three cycles.

Overall, the results discussed above show that the persistence characteristics of air pollutant concentrations in Mexico City are not constant over time and temporal scales. In fact, Hurst exponent variations reflect the complex way that diverse meteorological and socio-economical mechanisms have been influencing the behavior of air pollutant concentration in the recent 15 years.

Please cite this article in press as: M. Meraz, et al., Statistical persistence of air pollutants (O_3, SO_2, $NO_2$and PM_{10}) in Mexico City, Physica A (2015), http://dx.doi.org/10.1016/j.physa.2015.02.009

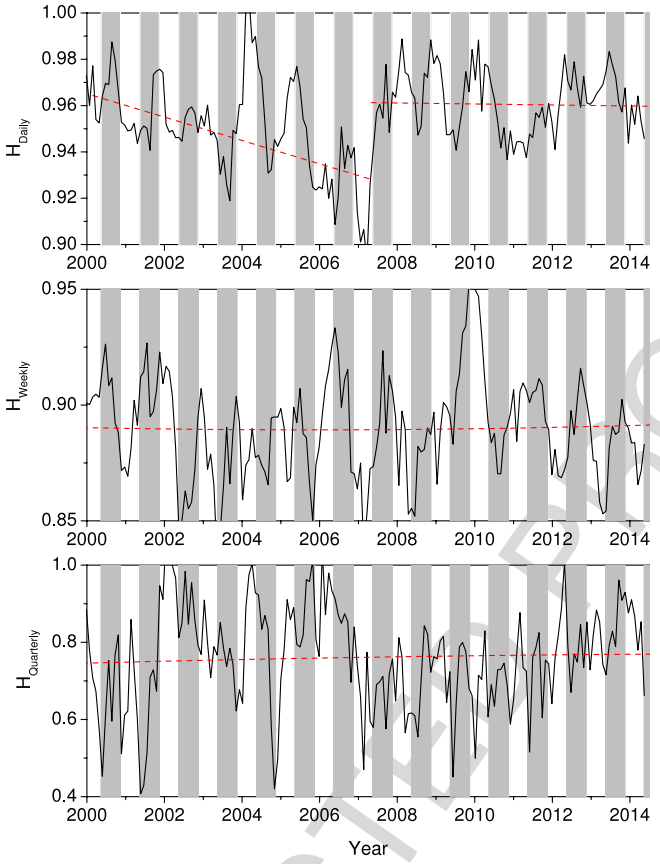

Fig. 12. Time variations of the Hurst exponent for small particles concentration, PM_{10}, over three different scales. The daily Hurst exponent exhibits a sudden increase in 2007.

5. Concluding remarks

This work used rescaled range (R/S) analysis for exploring the statistical persistence properties of four important air-pollutants (O_3, SO_2, NO_2 and PM_{10}) in Mexico City downtown. Persistence can be interpreted in terms of processes containing long-range memory effects. The results in this work showed that, on average, the dynamics of air-pollutants exhibit a persistent behavior, with small particles and ozone presenting the highest and the lowest persistence degree (quantified in terms of the Hurst exponent), respectively. However, it was also found that persistence is not a uniform property but exhibits scale dependence. This means that the predictability of air-pollutant dynamics depends strongly on the time scale. In this way, highest predictability (i.e., highest Hurst exponent) was detected for intraday and quarterly time scales, while reduced predictability was found for yearly time scales.

The long-term memory effects over a wide range of time scales should involve the complex interaction of diverse meteorological and socio-economic mechanisms acting at different time scales. For instance, meteorological mechanisms must be present over daily, quarterly and yearly time scales, while socio-economic mechanisms should be induced by weekly cycles of the socio-economic activity. How these mechanisms are interlaced in the accumulation of air-pollutants in Mexico City Metropolitan Area is an issue under the scrutiny of various local and abroad research groups. In fact, it has been argued that the air-pollutant dynamics in megacities like Mexico City can be interpreted from the framework of self-organized critically (SOC) systems [17,36]. Within the SOC framework, the frequency of occurrence of large pollution events is largely affected by minor air pollution events. In fact, the lack of a characteristic time scale underlying the pollutant dynamics might imply that, under adequate meteorological conditions, minor air pollution sources can trigger the occurrence of large pollution events. In fact, self-organized systems store material and/or energy for some time and release it once a critical level is reached [36]. It has been highlighted that minor pollution sources (e.g., restaurants, hotels, etc.) should be also accounted for modeling air-pollutant dynamics [15,17].

Overall, the analysis of persistence of time series can be considered as a complementary tool for monitoring the probable impact of air-pollution control measures in Mexico City. In fact, the application of new policies (e.g., changes in fuel, phasing out of older vehicles and the development of constrained lanes for public transport) aimed at reducing pollutant emissions should be reflected in both time-wise pollutant concentrations and their statistical persistence properties. Future work should address the analysis of other monitoring stations deployed in different zones of the MCMA.

Please cite this article in press as: M. Meraz, et al., Statistical persistence of air pollutants (O_3, SO_2, $NO_2$and PM_{10}) in Mexico City, Physica A (2015), http://dx.doi.org/10.1016/j.physa.2015.02.009

References

[1] L.T. Molina, M.J. Molina, Air Quality in the Mexico Megacity: An Integrated Assessment, Kluwer Academic Publishers, Dordrecht, The Netherlands, 2002.
[2] S. Orta-García, F. Pérez-Vázquez, C. González-Vega, J.A. Varela-Silva, L. Hernández-González, I. Pérez-Maldonado, Concentrations of persistent organic pollutants (POPs) in human blood samples from Mexico City, Mexico, Sci. Total Environ. 472 (2014) 496–501.
[3] M.L. Bell, D.L. Davis, N. Gouveia, V.H. Borja-Aburto, L.A. Cifuentes, The avoidable health effects of air pollution in three Latin American cities: Santiago, Sao Paulo, and Mexico City, Environ. Res. 100 (2006) 431–440.
[4] O. Morton-Bermea, E. Hernández-Álvarez, G. González-Hernández, F. Romero, R. Lozano, L.E. Beramendi-Orosco, Assessment of heavy metal pollution in urban topsoils from the metropolitan area of Mexico City, J. Geochem. Explor. 101 (2009) 218–224.
[5] P. Perez, A. Trier, Prediction of NO and NO_2 concentrations near a street with heavy traffic in Santiago, Chile, Atmos. Environ. 35 (2001) 1783–1789.
[6] A. Russo, F. Raischel, P.G. Lind, Air quality prediction using optimal neural networks with stochastic variables, Atmos. Environ. 79 (2013) 822–830.
[7] S. Osowski, K. Garanty, Forecasting of the daily meteorological pollution using wavelets and support vector machine, Eng. Appl. Artif. Intell. 20 (2007) 745–755.
[8] J. Brandt, J.D. Silver, L.M. Frohn, C. Geels, A. Gross, A.B. Hansen, K.M. Hansen, G.B. Hedegaard, C.A. Skjøth, H. Villadsen, A. Zare, J.H. Christensen, An integrated model study for Europe and North America using the Danish Eulerian Hemispheric Model with focus on intercontinental transport of air pollution, Atmos. Environ. 53 (2012) 156–176.
[9] F.J. Valdés-Parada, J.R. Varela, J. Alvarez-Ramirez, Upscaling pollutant dispersion in the Mexico City Metropolitan Area, Physica A 391 (2012) 606–615.
[10] D.M. Broday Yuval, Studying the time scale dependence of environmental variables predictability using fractal analysis, Environ. Sci. Technol. 44 (2010) 4629–4634.
[11] C. Varotsos, J. Ondov, M. Efstathiou, Scaling properties of air pollution in Athens, Greece and Baltimore, Maryland, Atmos. Environ. 39 (2005) 4041–4047.
[12] C.A. Varotsos, J.M. Ondov, A.P. Cracknell, M.N. Efstathiou, M.-N. Assimakopoulos, Long-range persistence in global Aerosol Index dynamics, Int. J. Remote Sens. 27 (2006) 3593–3603.
[13] S. Kai, L. Chun-qiong, A. Nan-shan, Z. Xiao-hong, Using three methods to investigate time-scaling properties in air pollution indexes time series, Nonlinear Anal. RWA 9 (2008) 693–707.
[14] H.L. Windsor, R. Toumi, Scaling and persistence of UK pollution, Atmos. Environ. 35 (2001) 4545–4556.
[15] A.B. Chelani, Statistical persistence analysis of hourly ground level ozone concentrations in Delhi, Atmos. Res. 92 (2009) 244–250.
[16] I.A. Pérez, M.L. Sánchez, M.A. García, V. Paredes, Persistence analysis of CO_2 concentrations recorded at a rural site in the upper Spanish plateau, Atmos. Res. 100 (2011) 45–50.
[17] K. Shi, C.Q. Liu, Self-organized criticality of air pollution, Atmos. Environ. 43 (2009) 3301–3304.
[18] C. Varotsos, M. Efstathiou, C. Tzanis, D. Deligiorgi, On the limits of the air pollution predictability: the case of the surface ozone at Athens, Greece, Environ. Sci. Pollut. Res. 19 (2012) 295–300.
[19] H.E. Hurst, R.P. Black, Y.M. Simaika, Long-Term Storage: An Experimental Study, Constable, London, 1965.
[20] B.B. Mandelbrot, J.R. Wallis, Computer experiments with fractional noises. part 1 averages and variances, Water Resour. Res. 5 (1969) 242–259.
[21] B. Qian, K. Rasheed, Hurst exponent and financial market predictability, in: M. Hamza (Ed.), Financial Engineering and Applications, FEA 2004, November 8–10, 2004, MIT, Cambridge, 2004.
[22] A. Chamoli, A.R. Bansal, V.P. Dimri, Wavelet and rescaled range approach for the Hurst coefficient for short and long time series, Comput. Geosci. 33 (2007) 83–93.
[23] R. Zuo, Q. Cheng, Q. Xia, Application of fractal models to characterization of vertical distribution of geochemical element concentration, J. Geochem. Explor. 102 (2009) 37–43.
[24] A.M. Churilla, W.A. Gottschalke, L.S. Liebovitch, L.Y. Selector, A.L. Todorov, S. Yeandle, Membrane potential fluctuations of human T-lymphocytes have fractal characteristics of fractional Brownian motion, Ann. Biomed. Eng. 24 (1996) 99–108.
[25] J.C. Echeverria, M.S. Woolfson, J.A. Crowe, B.R. Hayes-Gill, G.D.H. Croaker, H. Vyas, Interpretation of heart rate variability via detrended fluctuation analysis and $\alpha\beta$ filter, Chaos 13 (2003) 467–475.
[26] J. Alvarez-Ramirez, J. Alvarez, E. Rodriguez, G. Fernandez-Anaya, Time-varying Hurst exponent for US stock markets, Physica A 387 (2008) 6159–6169.
[27] A.W. Lo, Long-term memory in stock market prices, Econometrica 59 (1991) 1279–1313.
[28] R.B. Davies, D.S. Harte, Tests for Hurst effect, Biometrika 74 (1987) 95–101.
[29] D. Maraun, H.W. Rust, J. Timmer, Tempting long-memory-on the interpretation of DFA results, Nonlinear Processes Geophys. 11 (2004) 495–503.
[30] B.M. Tabak, D.O. Cajueiro, Are the crude oil markets becoming weakly efficient over time? a test for time-varying long-range dependence in prices and volatility, Energy Econ. 29 (2007) 28–36.
[31] C.A. Varotsos, M.N. Efstathiou, A.P. Cracknell, Plausible reasons for the inconsistencies between the modeled and observed temperatures in the tropical troposphere, Geophys. Res. Lett. 40 (2013) 4906–4910.
[32] C.A. Varotsos, M.N. Efstathiou, Is there any long-term memory effect in the tropical cyclones? Theor. Appl. Climatol. 114 (2013) 643–650.
[33] A.B. Chelani, Nonlinear dynamical analysis of ground level ozone concentrations at different temporal scales, Atmos. Environ. 44 (2010) 4318–4324.
[34] P. Lenschow, H.-J. Abraham, K. Kutzner, M. Lutz, J.D. Preuß, W. Reichenbächer, Some ideas about the sources of PM10, Atmos. Environ. 35 (2001) S23–S33.
[35] B. Ye, X. Ji, H. Yang, X. Yao, C.K. Chan, S.H. Cadle, T. Chan, P.A. Mulawa, Concentration and chemical composition of PM2.5 in Shanghai for a 1-year period, Atmos. Environ. 37 (2003) 499–510.
[36] P. Bak, C. Tang, K. Wiesenfeld, Self-organized criticality: an explanation of the 1/f noise, Phys. Rev. Lett. 59 (1987) 381–384.

Please cite this article in press as: M. Meraz, et al., Statistical persistence of air pollutants (O_3, SO_2, $NO_2$and PM_{10}) in Mexico City, Physica A (2015), http://dx.doi.org/10.1016/j.physa.2015.02.009